CrossMark

An adaptive neuro-fuzzy inference system for predicting unconfined compressive strength and Young's modulus: a study on Main Range granite

Danial Jahed Armaghani · Edy Tonnizam Mohamad ·
Ehsan Momeni · Mogana Sundaram Narayanasamy ·
Mohd For Mohd Amin

Abstract Engineering properties of rocks such as unconfined compressive strength (UCS) and Young's modulus (E) are among the essential parameters for the design of tunnel excavations. Many attempts have been made to develop indirect methods of estimating UCS and E. This is generally attributed to the difficulty of preparing and conducting the aforementioned tests in a laboratory. In essence, this study aims to present two predictive models of UCS and E for granite using an adaptive neuro-fuzzy inference system (ANFIS). The required rock samples for model development (45 granite sample sets) were obtained from site investigation work at the Pahang-Selangor raw water transfer tunnel, which was excavated across the Main Range of Peninsular Malaysia. In developing the predictive models, dry density, ultrasonic velocity, quartz content and plagioclase were set as model inputs. These parameters were selected based on simple and multiple regression analyses presented in the article. However, for the sake of comparison, the prediction performances of the ANFIS models were checked against multiple regression analysis (MRA) and artificial neural network (ANN) predictive models of UCS and E. The capacity performances of the predictive models were assessed based on the value account for (VAF), root mean squared error (RMSE) and coefficient of determination (R^2). It was found that the ANFIS predictive model of UCS, with R^2, RMSE and VAF equal to 0.985, 6.224 and 98.455 %, respectively, outperforms the MRA and ANN models. A similar conclusion was drawn for the ANFIS predictive model of E where the values of R^2, RMSE and VAF were 0.990, 3.503 and 98.968 %, respectively.

Introduction

Proper determination of unconfined compressive strength (UCS) and Young's modulus (E) of rocks is of crucial importance in the design of geotechnical engineering structures such as dams and tunnels. The latter is a key parameter in deformation analysis and the former gives good estimation of the rock bearing capacity. In other words, inappropriate estimation of the aforementioned rock parameters, i.e. UCS and E, could be catastrophic as it can lead to underestimation of the ultimate bearing capacity as well as the load corresponding to an allowable settlement for a problem of interest. The unconfined compression test is a laboratory test normally used to determine elastic modulus and strength of the rock. The test is conducted using standard procedures such as those of the International Society for Rock Mechanics (ISRM). However, there are

D. Jahed Armaghani (✉) · E. Tonnizam Mohamad ·
E. Momeni · M. F. Mohd Amin
Department of Geotechnics and Transportation, Faculty of Civil
Engineering, Universiti Teknologi Malaysia (UTM),
81310 Skudai, Johor, Malaysia
e-mail: danialarmaghani@yahoo.com

E. Tonnizam Mohamad
e-mail: edy@utm.my

E. Momeni
e-mail: mehsan23@live.utm.my

M. F. Mohd Amin
e-mail: mohdfor@utm.my

M. S. Narayanasamy
Aurecon Pty Ltd, Brisbane, Australia
e-mail: mogana.sundaram@aurecongroup.com

some impeding factors in direct determination of UCS and E in the laboratory. For instance, preparing the required rock core samples is often difficult, especially for rocks that are highly fractured and those that exhibit significant lamination and foliation (Singh et al. 2012; Monjezi et al. 2012). At preliminary design stage, direct determination of UCS and E can be too expensive and time consuming (Yilmaz and Sendir 2002; Gokceoglu and Zorlu 2004; Kahraman 2014). Nevertheless, alternative and indirect approaches of predicting the rock strength and modulus are available, such as traditional and multiple regression models and soft computing techniques.

Many attempts have been made in developing conventional (also called indirect) methods of UCS or E estimation. These alternative methods for predicting UCS and E, are often in forms of simple regression between UCS or E and simple index tests of rocks such as the Schmidt hammer (Singh et al. 1983; Yasar and Erdogan 2004; Nazir et al. 2013b; Karaman and Kesimal 2014), ultrasonic velocity, or V_p (Kahraman 2001; Cobanglu and Celik 2008), Brazilian tensile strength (Gokceoglu and Zorlu 2004; Kahraman et al. 2012; Nazir et al. 2013a), point-load index (Sulukcu and Ulusay 2001; Basu and Aydin 2006; Tandon and Gupta 2014) and slake durability index (Moradian et al. 2010; Yagiz 2011) tests.

In addition, some researchers addressed the successful application of multiple regression analysis (MRA) in predicting rock strength and module of elasticity (Gokceoglu and Zorlu 2004; Yilmaz and Yuksek 2009). However, there are some reported cases where these correlations are found to be insufficient to provide highly reliable values of the UCS and E (Dehghan et al. 2010; Beiki et al. 2013). In general, the use of these equations is recommended only for specific rock types (Beiki et al. 2013). Furthermore, statistical prediction methods suffer from a disadvantage in respect to new available data: If different from the original data, the form of the obtained equations needs to be updated (O'Rourke 1989; Rezaei et al. 2012).

Recent studies have highlighted the application of soft computation techniques such as the artificial neural network (ANN) and the adaptive neuro-fuzzy inference system (ANFIS) in geotechnical engineering problems. This is attributed to the well-established fact that soft computation techniques are feasible, quick and promising tools for the solving of engineering problems, particularly when the contact natures between independent variables and dependent variables are unknown (Garret 1994; Yilmaz and Yuksek 2009; Atici 2011; Rezaei et al. 2012; Asadi et al. 2013; Yesiloglu-Gultekin et al. 2013; Marto et al. 2014; Momeni et al. 2014a). Also from an economic point of view, implementation of these techniques is advantageous as direct or indirect determination of UCS or E in the laboratory is relatively costly.

This article presents an ANFIS model for prediction of UCS and E for Main Range granite in Malaysia. For comparative purposes, the prediction performance of the ANFIS model is compared with the ANN model and MRA.

Previous investigations

Numerous researchers have been working on the prediction of UCS using soft computing methods. Meulenkamp and Grima (1999) predicted UCS using a back propagation (BP) neural network. They used 194 different types of rock samples including sandstone, limestone, dolomite and others. In their study, Equotip hardness reading, density, porosity, rock type and grain size were considered as inputs for UCS prediction. According to their conclusion, the ANN is able to generalise much better than statistical models. Sonmez et al. (2004) used a fuzzy inference system (FIS) and regression techniques for prediction of UCS and the elasticity modulus based on petrographic data from 164 samples of Ankara agglomerate. Based on their findings, fuzzy logic can provide high performance prediction capacity to determine UCS; however, their findings suggest that, for predicting E, the regression equations are more suitable. In another study, Gokceoglu and Zorlu (2004) implemented fuzzy model and regression techniques to predict the UCS and E of problematic rocks. The point load index, block punch index, ultrasonic velocity and tensile strength of 82 samples were considered as inputs in their predictive models. They concluded that the fuzzy model provides the most reliable predictions when compared with the simple and multiple regression models. Dehghan et al. (2010) used feed forward neural network and regression analyses to predict UCS and E. In their study, some rock index parameters such as point load index, p-wave (ultrasonic) velocity, porosity and Schmidt hammer rebound number were considered as inputs to predict UCS and E for 30 travertine rock data sets. They concluded that the ANN method outperforms regression analyses. Mishra and Basu (2013) applied MRA and FIS models for the estimation of UCS in three different rocks and compared the results of these methods with simple regression. They found that both the MRA and FIS models exhibited better predictive performances compared to the MRA model. Cevik et al. (2011) reported the feasibility of ANN in predicting the UCS of sedimentary rock samples. In their model, the origin of rocks, two/four-cycle slake durability indices and clay contents of 56 rock sample sets were set as inputs for prediction of UCS. In another study, Yesiloglu-Gultekin et al. (2013) suggested the superiority of the ANFIS model compared to the ANN model and MRA in predicting the UCS of granite samples in Turkey. They used 75 rock sample sets in the development of their predictive models.

Overall, the inputs of their proposed predictive models of UCS included the rock tensile strength, block punch index, point load index and p-wave velocity. Finally, they recommended that the best ANFIS prediction performance is expected when tensile strength and p-wave velocity values are used as model inputs.

Singh et al. (2001) proposed a number of correlations between strength parameters (UCS, axial point load strength and tensile strength) and some index parameters (mineral composition, grain size, aspect ratio, form factor, area weighting and orientation of foliation planes of weakness) of schistose rock. They used the petrographic properties to predict strength parameters using a BP neural network. Their findings show that the ANN prediction model is more accurate than the proposed correlations. A fuzzy triangular chart was utilised by Gokceoglu (2002) to predict UCS using the petrographic composition. To this end, he produced 15 membership functions for 15 data sets and showed that the FIS model is able to predict UCS values. The relationships between petrographic properties and strength of sandstone were investigated by Zorlu et al. (2008). They predicted the UCS of sandstone using MRA and ANN techniques. Comparison of the MRA and ANN models showed that the ANN model can predict UCS with a higher prediction capacity. Yagiz et al. (2012) developed ANN and nonlinear regression techniques to predict UCS and E of 54 carbonate rocks. They concluded that the ANN model

indicates better results in predicting UCS and E compared to the nonlinear regression technique. Some recent studies on the prediction of UCS and E using soft computation techniques are tabulated in Table 1.

Case study and test procedure

The rock samples for the current study were collected from a water transfer tunnel project. The tunnel was designed to transfer raw water from the Semantan River in Pahang State to Selangor State. This is to meet the additional water demands for Selangor state and Kuala Lumpur. The tunnel was excavated to cross the Main Range, which lies between Pahang and Selangor States. This mountain range forms the backbone of Peninsular Malaysia with elevation ranging from 100 to 1,400 m. The main rock type is granite, locally termed as Main Range granite, with typical intact strength between 150 and 200 MPa.

The tunnel is 44.6 km in length with a diameter of 5.2 m and a longitudinal gradient of 1/1,900. It is designed to operate under free flow conditions with a maximum discharge of 27.6 m^3/s of raw water. For tunnel excavation, a tunnel boring machine (TBM) was primarily used for about 35 km of the length throughout the main tunnel route, while the remaining tunnel portions, which include access work adits, were excavated using the conventional drill and blast method. Three TBM sections and four conventional

Table 1 Recent works on UCS and E prediction using soft computation techniques

References	Technique	Input	Output	R^2 or R
Meulenkamp and Grima (1999)	ANN	L, n, ρ, d	UCS	$R = 0.97$
Singh et al. (2001)	ANN	PSV	UCS, BTS, APLS	–
Gokceoglu and Zorlu (2004)	FIS	Is(50), BPI, V_p, BTS	USC, E	$R = 0.82$
Zorlu et al. (2008)	ANN	q, pd, cc	UCS	$R = 0.87$
Yilmaz and Yuksek (2009)	ANFIS	V_p, Is(50), SR_n, WC	UCS, E	$R^2_{UCS} = 0.94$ $R^2_E = 0.95$
Dehghan et al. (2010)	ANN	V_p, Is(50), SR_n, n	UCS, E	$R^2 = 0.86$
Majdi and Beiki (2010)	GA-ANN	ρ, RQD, n, NJ, GSI	E	$R^2 = 0.89$
Rabbani et al. (2012)	ANN	n, BD, S_w	UCS	$R = 0.98$
Singh et al. (2012)	ANFIS	ρ, Is(50), WA	E	$R^2 = 0.66$
Rezaei et al. (2012)	FIS	SR_n, ρ, n	UCS	$R^2 = 0.95$
Ceryan et al. (2012)	ANN	n, I_d, V_m, n_e, PSV	UCS	$R^2 = 0.88$
Yesiloglu-Gultekin et al. (2013)	ANFIS	BTS, V_p	UCS	$R^2 = 0.60$
Beiki et al. (2013)	GP	ρ, n, V_p	UCS, E	$R_{UCS} = 0.91$ $R_E = 0.82$
Momeni et al. (2014b)	PSO-ANN	ρ, V_p, Is(50), SR_n	UCS	$R^2 = 0.97$
Tonnizam Mohamad et al. (2014)	PSO-ANN	Is(50), BTS, BD, V_p	UCS	$R^2 = 0.97$

L equotip value, n porosity, ρ density, d grain size, PSV petrography study values, $APLS$ axial point load strength, BPI block punch index, V_p p-wave velocity, BD bulk density, S_w water saturation, I_d slake durability index, V_m p-wave velocity in solid part of the sample, n_e effective porosity, q quartz content, pd packing density, cc concavo convex, RQD rock quality designation, NJ number of joints per meter, GSI geological strength index, GA genetic algorithm, WC water content, GP genetic programming, WA water absorption, PSO particle swarm optimization
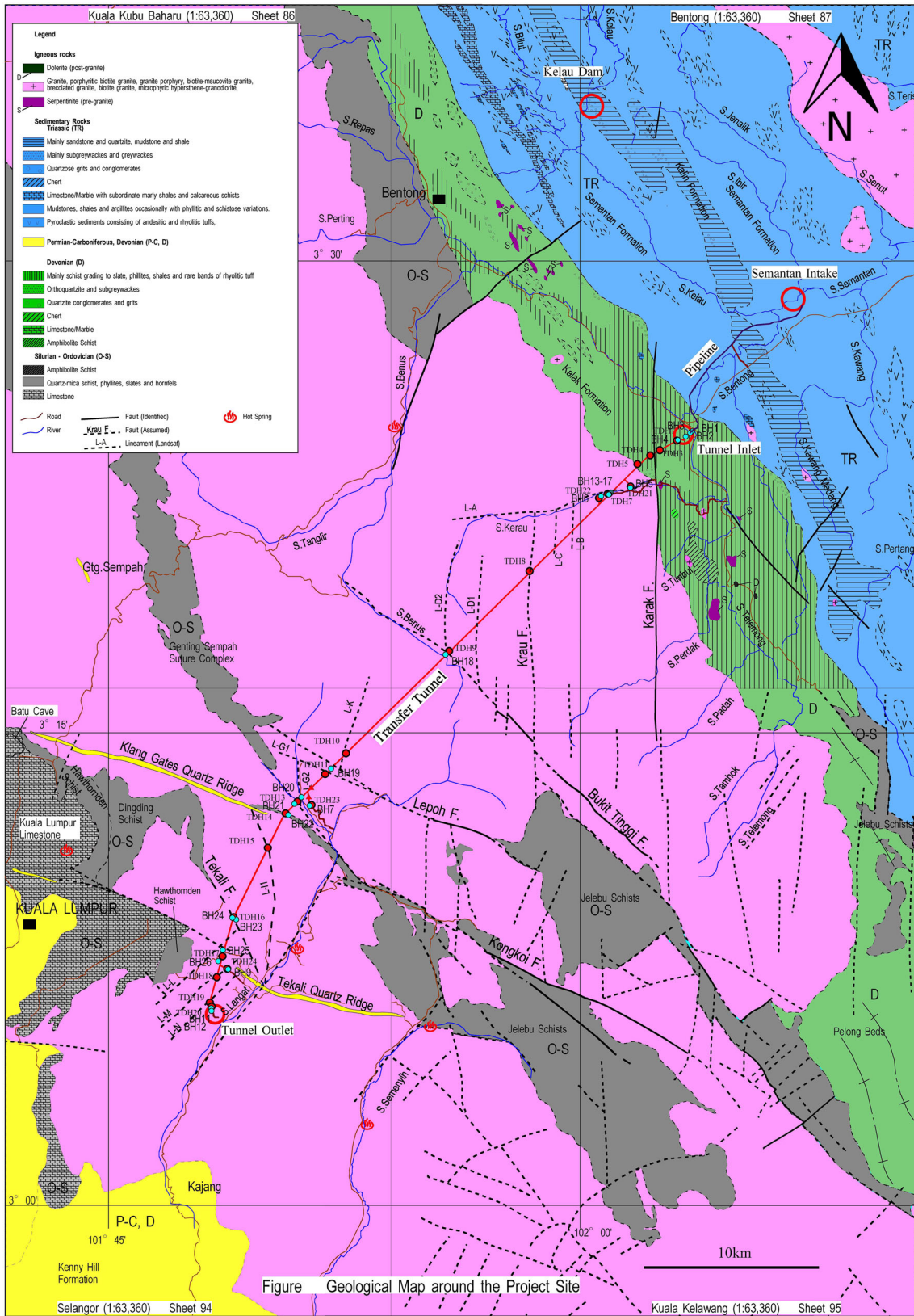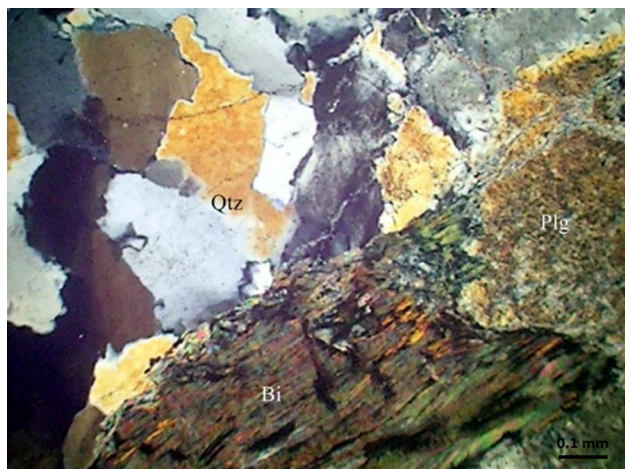
Fig. 1 Geological map around the tunnel site

Fig. 2 Thin-section photomicrograph of sample BH23_67.45–67.60

drill and blast sections were planned for excavation of this tunnel. Figure 1 shows the geological map around the tunnel site and also displays the location of boreholes.

Selected borehole core samples were transported to a laboratory to verify the relevant engineering and physical properties of the granite. The end surfaces of the trimmed cores were carefully lapped to obtain the required finishing and shape. A total of 45 granite rock samples were prepared for the laboratory tests. Samples were checked for any existing cracks and other small-scale discontinuities that may lead to an undesirable variation in properties and premature failures. The rock physical properties tested include dry density (ρ_{dry}) and V_p. Additionally, uniaxial compression tests were performed to determine the UCS and E of the granite. Knowing the axial strain as well as the stress measured through relevant transducers, the Young's moduli of rock samples were measured. All test and sample preparation procedures were conducted in accordance with ISRM (2007) standards.

Petrographic analyses of the granite samples were also carried out using a polarizing petrological microscope. For this purpose, thin sections of the samples were prepared to identify the percentage of different minerals; some photomicrograph results are shown in Fig. 2. The samples exhibit holocrystalline and non-porphyritic mineral texture, and in general mainly consist of interlocking coarse-grained crystals of quartz (Qtz), alkali feldspar (Kpr), plagioclase (Plg) and biotite (Bi). Such texture is typical of plutonic igneous rock. The test results of all 45 data sets are tabulated in Table 2. Note that micas are represented by three minerals: muscovite, biotite and sericite.

Data analyses

In order to analyze the laboratory test results, different statistical and simulation techniques were employed in this study. The following sections describe implementation of the aforementioned methods to predict the UCS and E of granite samples. Subsequently, the values of UCS and E obtained from laboratory tests were compared with the corresponding predicted values of UCS and E.

Simple regression

In this study, simple regression analysis was initially undertaken in order to establish the predictive equations between independent or input variables (ρ_{dry}, V_p, Qtz, Kpr, Mica, Chl and Plg) and dependent or output variables (UCS and E). The relationships between UCS and E with input parameters were analyzed and some linear, exponential, logarithmic and power equations were proposed, as tabulated in Tables 3 and 4, respectively. The standard error and coefficient of determination (R^2) were used to evaluate the reliability of the obtained equations.

Multiple regression

Multiple regression analysis can be used to obtain the best-fit equation when there is more than one input parameter. The form of the MRA formula is $y = b_1 x_1 + b_2 x_2 + b_n x_n + c$, where {$b_1$, b_2,…, b_n} are the coefficients of regression, and c is a constant value of y when all input parameters are zero. The main theoretical weakness of all regression techniques is that they can only ascertain relationships, but never determine the exact underlying causal mechanism (Yilmaz and Yuksek 2009).

Many MRAs were carried out to predict UCS and E using different input parameters, as tabulated in Table 5. According to this table, the values of standard error as well as R^2 for both UCS and E are very close when different input parameters were used. It is worth mentioning that when these analyses were performed, the models with R^2 of more than 0.50 were taken into consideration. Nevertheless, the model number 8 in Table 5 was selected due to the fact that a predictive model with a lower number of inputs is of advantage as this can reduce the model complexity.

In total, it was found that, among all parameters presented in Table 2, ρ_{dry}, V_p, Qtz and Plg were better correlated with UCS and E. Therefore, these parameters were selected for the subsequent analyses. It should be mentioned that the statistical software package SPSS 18.0 was used for analysis of the MRA models. The obtained correlations using MRA analyses are presented in Eqs. 1 and 2:

$$\text{UCS} = 69.505\rho_{dry} + 0.025V_p - 0.479\,\text{Qtz} - 1.439\,\text{Plg} - 158.796, \tag{1}$$

$$E = -34.519\rho_{dry} + 0.019V_p + 1.217\,\text{Qtz} - 0.612\,\text{Plg} + 22.681. \tag{2}$$

Table 2 Mineralogical and other properties of the granite samples

Sample number	Sample name	Petrographic name	ρ_{dry} (g/cm^3)	V_p (m/s)	Qtz (%)	Kpr (%)	Plg (%)	Chl (%)	Mica (%)	UCS (Mpa)	E (Gpa)
1	TDH7_35.1–35.4	Microgranite	2.05	3,070	19	15	45	3	18	15	5.7
2	TDH7_38.2–38.4	Microgranite	2.21	3,440	16	14	51	2	15	26	13
3	TDH7_54.6–54.95	Coarse grained granite	2.35	3,660	22	35	28	5	10	39	13.1
4	TDH10_241.0–2411.3	Microgranite	2.72	4,860	32.1	33	22.4	2	10	144	52.7
5	TDH10_278.6–279.0	Microgranite	2.68	5,840	29.7	29	27.3	3	11	161	70.1
6	TDH10_305.7–306.0	Microgranite	2.68	5,830	29.3	25.2	32.5	0	13	176	73.2
7	TDH11_292.6–292.9	Medium grained granite	2.62	5,700	23.5	22.5	36	4	14	60	34.9
8	TDH13_124.1–124.5	Medium to coarse grained granite	2.65	5,370	29.4	28.2	31	0	11	132	50.9
9	TDH13_156.8–157.0	Medium to coarse grained granite	2.64	5,360	30.4	32	26	3	8	54	45.2
10	TDH15_113.7–113.9	Medium to coarse grained granite	2.7	5,260	30.5	35	22	4	8.5	133	61.7
11	TDH16_51.6–51.8	Medium to coarse grained granite	2.58	5,050	32	31	29	0	8	75	46.7
12	TDH17_43.2–43.6	Fine grained granite	2.62	5,420	27.9	31	30.1	0	11	38	30.3
13	TDH17_99.8–100.1	Medium to coarse grained granite	2.62	5,540	30.1	27	34	1	7.9	51	51.8
14	TDH18_52.1–52.4	Coarse grained granite	2.54	4,930	25.5	35	29.5	0	10	71	34.7
15	TDH18_67.3–67.5	Coarse grained granite	2.57	5,320	24	37	34	0	5	78	52.4
16	TDH19_125.0–125.2	Coarse grained granite	2.62	5,370	30.5	33	28.5	0	8	153	66.5
17	TDH19_130.6–131.0	Coarse grained granite	2.62	5,250	28.1	35	20	1	9	148	50.9
18	TDH20_43.5–43.8	Coarse grained granite	2.55	2,700	29.7	32.3	28	1	9	57	18.6
19	TDH20_44.5–44.8	Coarse grained granite	2.64	4,120	37.6	31.4	22	0	9	75	51.4
20	TDH20_48.5–48.8	Coarse grained granite	2.67	4,520	35.1	39.9	15	0	7	75	39.7
21	BH18_55.8–56.1	Bi granite	2.48	4,820	35	30	32	4	6	21.9	13.6
22	BH18_295.6–295.9	Leucogranite	2.72	6,570	30	39	22	4	6	54.7	35.6
23	BH19 _198.7–199.0	Porphyry granite	2.67	7,072	50	45	0	3	8	98	51.9
24	BH20_88.1–88.55	Coarse–grained protomylonite granite	2.6	4,427	35	35	20	3	8	124.5	59.4
25	BH20_93–93.6	Coarse–grained protomylonite granite	2.59	4,765	35	35	20	3	9	113	55
26	BH20 _94.4–94.7	Porphyritic bi granite	2.71	5,842	35	30	33	0	7	21.9	11.3
27	BH21_157.0–157.4	Coarse–grained protomylonite granite	2.53	4,385	35	35	19	0	7	47.3	22.5
28	BH21_158.4–158.8	Coarse–grained protomylonite granite	2.61	6,482	33	34	22	4	1	147.1	73.3
29	BH21_160.1–160.5	Coarse–grained protomylonite granite	2.64	4,450	33	35	19	4	1.5	128.6	60.6
30	BH21_165.0–165.4	Coarse–grained protomylonite granite	2.62	4,560	35	35	18	0	6	98	53.9
31	BH21_165.7–166.0	Bi granite	2.76	6,175	37	28	30	0	5	84.2	46.3
32	BH23_67.45–67.6	Coarse grained granite	2.58	4,707	33	31	29	0	5	85.3	43
33	BH23 _70.4–70.7	Bi granite	2.59	6,610	32	32	33	0	8	136.1	59
34	BH23_70.8–71.0	Coarse grained granite	2.6	4,385	33	31	29	0	8	96	65.7
35	BH24_52.1–52.5	Coarse grained granite	2.65	7,242	40	27	30	0	3	127.9	116.3
36	BH24_74.6–74.8	Coarse–grained protomylonite granite	2.62	5,402	36	32	27	0	3	73	53.6
37	BH24_78.75–78.95	Coarse–grained protomylonite granite	2.62	5,117	37	31	26	0	5	204.9	142.3
38	BH25_150–155	Coarse grained leucoggranite	2.58	5,525	37	31	27	2	9	130.9	130.9
39	BH25_155.5–155.9	Coarse grained leucoggranite	2.66	8,550	39	29	23	0	3	98.9	93.3
40	BH25_164.7–165.0	Bi granite	2.70	6,742	33	30	35	0	2	188.9	96.9
41	BH25_170–175	Coarse grained granite	2.59	5,497	35	33	26	0	9	183.9	90.1
42	BH26_160.7–160.95	Coarse grained granite	2.63	5,095	33	33	29	0	9	195.9	91.9
43	BH26_167.65–167.85	Coarse grained granite	2.65	5,305	33	32	26	0	5	156.8	100.6
44	BH26_172.8–173.0	Coarse grained granite	2.76	7,702	34	28	29	0	5	146.9	74.9
45	BH26_173.55–173.75	Coarse grained granite	2.65	5,370	32	31	29	0	2	85.9	55.1

Qtz quartz, *Kpr* alkali feldspar, *Plg* plagioclase, *Chl* chlorite

Table 3 Results of simple regression analyses for UCS prediction

Regression model	Predictor	Regression function	SE	R^2
Linear	ρ_{dry}	$\text{UCS} = 240.9 \times \rho_{dry} - 524.61$	41.69	$R^2 = 0.354$
	V_p	$\text{UCS} = 0.0308 \times E - 61.602$	37.82	$R^2 = 0.468$
	Plg	$\text{UCS} = -2.4683 \times \text{Plg} + 169.63$	48.01	$R^2 = 0.143$
	Qtz	$\text{UCS} = 4.3006 \times \text{Qtz} - 35.371$	45.61	$R^2 = 0.227$
	Kpr	$\text{UCS} = 2.3968 \times \text{Kpr} + 27.193$	50.21	$R^2 = 0.063$
	Mica	$\text{UCS} = -3.563 \times \text{Mica} + 129.63$	50.25	$R^2 = 0.0611$
	Chl	$\text{UCS} = -6.718 \times \text{Chl} + 110.84$	50.63	$R^2 = 0.0469$
Exponential	ρ_{dry}	$\text{UCS} = 0.0111e^{3.4437 \times \rho_{dry}}$	40.33	$R^2 = 0.4721$
	V_p	$\text{UCS} = 12.861e^{0.0004 \times V_p}$	54.42	$R^2 = 0.416$
	Plg	$\text{UCS} = 215.95e^{-0.033 \times \text{Plg}}$	50.24	$R^2 = 0.1707$
	Qtz	$\text{UCS} = 14.346e^{0.0563 \times \text{Qtz}}$	48.08	$R^2 = 0.2536$
	Kpr	$\text{UCS} = 23.548e^{0.0417 \times \text{Kpr}}$	52.58	$R^2 = 0.1237$
	Mica	$\text{UCS} = 140.6e^{-0.063 \times \text{Mica}}$	52.82	$R^2 = 0.124$
	Chl	$\text{UCS} = 97.913e - 0.094 \times \text{Chl}$	52.77	$R^2 = 0.0595$
Logarithmic	ρ_{dry}	$\text{UCS} = 568.87\ln(\rho_{dry}) - 441.05$	42.26	$R^2 = 0.3361$
	V_p	$\text{UCS} = 154.87\ln(V_p) - 1,222.6$	38.51	$R^2 = 0.4487$
	Plg	–	–	–
	Qtz	$\text{UCS} = 125.82\ln(\text{Qtz}) - 331.65$	45.62	$R^2 = 0.2265$
	Kpr	$\text{UCS} = 69.192\ln(\text{Kpr}) - 134.81$	49.86	$R^2 = 0.0759$
	Mica	$\text{UCS} = -19.95\ln(\text{Mica}) + 140.16$	50.42	$R^2 = 0.0551$
	Chl	–	–	–
Power	ρ_{dry}	$\text{UCS} = 0.0324 \times \rho_{dry}^{8.2646}$	40.79	$R^2 = 0.4635$
	V_p	$\text{UCS} = 9E{-}06 \times V_p^{1.8797}$	39.25	$R^2 = 0.4318$
	Plg	–	–	–
	Qtz	$\text{UCS} = 0.2198 \times \text{Qtz}^{1.7339}$	47.23	$R^2 = 0.281$
	Kpr	$\text{UCS} = 1.2129 \times \text{Kpr}^{1.2465}$	52.34	$R^2 = 0.1608$
	Mica	$\text{UCS} = 157.15 \times \text{Mica}^{-0.312}$	52.85	$R^2 = 0.0881$
	Chl	–	–	–

Model summaries of MRA for prediction of UCS and E are illustrated in Table 6.

Artificial neural network

The ANN is an artificial intelligence technique that has been demonstrated to solve many composite engineering problems successfully. It is an information-processing system in which system information is processed by several interconnected simple elements that are known as nodes or neurons, positioned in the network layers. The best ANN has been identified as the multilayer perceptron (MLP) model, which is composed of three different layers: input, output and hidden layers (Dreyfus 2005; Jahed Armaghani et al. 2013). The nodes are linked from one layer to the next, but this connection is not within the same layer. After processing the information, the connection links transmit the information between the neurons. A weight is assigned to each link, which is multiplied into the transmitted signal. The total weighted input signal of each node is usually transmitted via a nonlinear activation function.

Performance of an ANN is directly dependent on the architecture of layers and the number of neurons, which is the pattern of the connections between the neurons (Haji-hassani et al. 2014). The BP algorithm is considered the most popular and effective learning algorithm for multilayered networks (Tawadrous and Katsabanis 2007). In BP, the connection weights are adjusted to reduce the errors of output (Jahed Armaghani et al. 2014). Initially, the network runs with connection weights that are selected randomly. In a feed-forward (FF) BP algorithm, the signals flow from the input layer to the output layer. Finally, a desired output is computed by the network, and then the difference between the actual outputs and the desired one is calculated. Network error is defined as the difference between the real values and those predicted by the system. The network error in each step is propagated back, and the individual weights are updated accordingly. This process is iterated until the error converges to a level that is known by some cost functions, such as root mean squared error (RMSE) (Simpson 1990; Kosko

Table 4 Results of simple regression analyses for E prediction

Regression model	Predictor	Regression function	SE	R^2
Linear	ρ_{dry}	$E = 122.45 \times \rho_{\mathrm{dry}} - 261.86$	26.59	$R^2 = 0.2579$
	V_{p}	$E = 0.0205 \times E - 52.172$	19.91	$R^2 = 0.5841$
	Plg	$E = -1.4884 \times \mathrm{Plg} + 97.395$	28.51	$R^2 = 0.1469$
	Qtz	$E = 3.1926 \times \mathrm{Qtz} - 45.433$	24.84	$R^2 = 0.3526$
	Kpr	$E = 1.6533 \times \mathrm{Kpr} + 4.9675$	29.54	$R^2 = 0.0842$
	Mica	$E = -3.4603 \times \mathrm{Mica} + 83.268$	28.25	$R^2 = 0.1628$
	Chl	$E = -5.2007 \times \mathrm{Chl} + 63.372$	29.62	$R^2 = 0.0794$
Exponential	ρ_{dry}	$E = 0.0025e^{3.7843 \times \rho_{\mathrm{dry}}}$	26.66	$R^2 = 0.5015$
	V_{p}	$E = 4.4295e^{0.0004 \times V_{\mathrm{p}}}$	27.39	$R^2 = 0.5635$
	Plg	$E = 122.9e^{-0.035 \times \mathrm{Plg}}$	29.41	$R^2 = 0.1641$
	Qtz	$E = 4.8629e^{0.0712 \times \mathrm{Qtz}}$	25.76	$R^2 = 0.3567$
	Kpr	$E = 10.93e^{0.0468 \times \mathrm{Kpr}}$	30.69	$R^2 = 0.1376$
	Mica	$E = 95.612e^{-0.092 \times \mathrm{Mica}}$	29.67	$R^2 = 0.2319$
	Chl	$E = 55.754e^{-0.127 \times \mathrm{Chl}}$	30.86	$R^2 = 0.0966$
Logarithmic	ρ_{dry}	$E = 291.69\ln(\rho_{\mathrm{dry}}) - 221.8$	26.75	$R^2 = 0.2495$
	V_{p}	$E = 103.25\ln(V_{\mathrm{p}}) - 826.52$	20.41	$R^2 = 0.563$
	Plg	–	–	–
	Qtz	$E = 89.529\ln(\mathrm{Qtz}) - 252$	25.39	$R^2 = 0.3237$
	Kpr	$E = 44.836\ln(\mathrm{Kpr}) - 96.858$	29.45	$R^2 = 0.0899$
	Mica	$E = -18.2\ln(\mathrm{Mica}) + 91.288$	28.81	$R^2 = 0.1295$
	Chl	–	–	–
Power	ρ_{dry}	$E = 0.0077 \times \rho_{\mathrm{dry}}^{9.1431}$	26.58	$R^2 = 0.499$
	V_{p}	$E = 7E{-}08 \times V_{\mathrm{p}}^{2.3748}$	21.78	$R^2 = 0.6063$
	Plg	–	–	–
	Qtz	$E = 0.0278 \times \mathrm{Qtz}^{2.1575}$	25.25	$R^2 = 0.3826$
	Kpr	$E = 0.3877 \times \mathrm{Kpr}^{1.4027}$	30.69	$R^2 = 0.1791$
	Mica	$E = 110.14 \times \mathrm{Mica}^{-0.444}$	30.82	$R^2 = 0.1569$
	Chl	–	–	–

1994). The scenario for the pth pattern in an FF neural network is presented in the following steps:

1. The ith node in the input layer holds a value of x_{pi} for the pth pattern.
2. Net input to the jth neuron in the hidden layer for pattern p is:

$$\mathrm{net}_{pj} = \sum_{i}^{N} W_{ij}O_{pi}, \tag{3}$$

where W_{ij} is the weight from node i to j. The output from each unit j is the threshold function, f_j, which acts on the weighted sum. In this MLP model, f_j is the sigmoid function as follows:

$$f(\mathrm{net}) = 1/(1 + e^{-K_{\mathrm{net}}}); (0 < f(\mathrm{net}) < 1), \tag{4}$$

where k is a positive constant that controls the function spread.

3. Output of the jth node is defined as:

$$O_{pj} = f_j(\mathrm{net}_{pj}). \tag{5}$$

4. Net input to the kth neuron of the output layer is:

$$\mathrm{net}_k = \sum_{j}^{N} W_{kj}X_{pj}, \tag{6}$$

where W_{kj} is the weight value between the kth output layer node and the ith hidden layer.

5. Output of the kth node of the output layer is:

$$O_{pk} = f_k(\mathrm{net}_k). \tag{7}$$

6. E_p is the function error for a pattern, p:

$$E_p = \frac{1}{2}\sum_{k}^{N}(t_{pk} - O_{pk})^2, \tag{8}$$

where O_{pk} and t_{pk} are the real and target outputs for pattern p on neuron k, respectively.

As mentioned previously, ρ_{dry}, V_{p}, Qtz and Plg were selected as model inputs to predict UCS and E. In this study, all 45 data sets were randomly distributed into two different data set categories, namely training and testing. In

Table 5 Results of multiple regression analyses for UCS and E

Model no.	Input	Output	SE		R^2	
			UCS	E	UCS	E
1	ρ_{dry}, V_p, Qtz	UCS, E	36.64	18.54	0.524	0.656
2	ρ_{dry}, V_p, Kpr	UCS, E	36.79	19.44	0.520	0.622
3	ρ_{dry}, V_p, Plg	UCS, E	35.87	18.76	0.544	0.648
4	ρ_{dry}, V_p, Chl	UCS, E	36.72	20.32	0.522	0.587
5	ρ_{dry}, V_p, Mica	UCS, E	36.64	19.88	0.524	0.604
6	ρ_{dry}, V_p, Qtz, Mica	UCS, E	36.39	18.77	0.542	0.656
7	ρ_{dry}, V_p, Qtz, Kpr	UCS, E	37.08	18.53	0.524	0.664
8	ρ_{dry}, V_p, Qtz, Plg	UCS, E	36.27	18.48	0.545	0.667
9	ρ_{dry}, V_p, Qtz, Chl	UCS, E	36.93	18.75	0.528	0.656
10	ρ_{dry}, V_p, Kpr, Plg	UCS, E	35.57	18.98	0.562	0.648
11	ρ_{dry}, V_p, Kpr, Mica	UCS, E	36.84	19.57	0.530	0.626
12	ρ_{dry}, V_p, Kpr, Chl	UCS, E	37.11	19.68	0.523	0.621
13	ρ_{dry}, V_p, Plg, Mica	UCS, E	35.96	18.67	0.552	0.659
14	ρ_{dry}, V_p, Mica, Chl	UCS, E	36.96	20.12	0.527	0.605
15	ρ_{dry}, V_p, Qtz, Kpr, Plg	UCS, E	35.83	18.69	0.567	0.667
16	ρ_{dry}, V_p, Qtz, Kpr, Chl	UCS, E	37.39	18.76	0.529	0.665
17	ρ_{dry}, V_p, Qtz, Kpr, Mica	UCS, E	36.75	18.75	0.545	0.665
18	ρ_{dry}, V_p, Plg, Mica, Chl	UCS, E	36.41	18.85	0.533	0.661
19	ρ_{dry}, V_p, Qtz, Plg, Mica	UCS, E	36.39	18.67	0.553	0.668
20	ρ_{dry}, V_p, Kpr, Plg, Mica	UCS, E	35.99	18.72	0.563	0.666
21	ρ_{dry}, V_p, Qtz, Kpr, Chl, Mica	UCS, E	37.01	18.99	0.548	0.665
22	ρ_{dry}, V_p, Qtz, Kpr, Mica, Plg	UCS, E	36.18	18.91	0.569	0.668
23	ρ_{dry}, V_p, Qtz, Kpr, Chl, Plg	UCS, E	36.24	18.93	0.568	0.667
24	ρ_{dry}, V_p, Qtz, Mica, Chl, Plg	UCS, E	36.85	18.91	0.554	0.669
25	ρ_{dry}, V_p, Kpr, Mica, Chl, Plg	UCS, E	36.46	18.84	0.563	0.670
26	ρ_{dry}, V_p, Qtz, Kpr, Mica, Chl, Plg	UCS, E	36.27	19.11	0.579	0.671

Table 6 Model summaries of the MRA model for prediction of UCS and E

Independent variable	Coefficients	SE	t value	p value
For UCS				
Constant	−158.796	162.835	−0.975	0.335
ρ_{dry}	69.505	63.632	1.092	0.281
V_p	0.025	0.006	3.859	0.000
Qtz	−0.479	1.5891	−0.302	0.764
Plg	−1.439	1.062	−1.354	0.183
For E				
Constant	22.681	82.942	0.273	0.786
ρ_{dry}	−34.519	32.412	−1.065	0.293
V_p	0.019	0.003	5.714	0.000
Qtz	1.217	0.809	1.504	0.141
Plg	−0.612	0.541	−1.131	0.264

Table 7 The proposed number of neurons for the hidden layer

Heuristic	References
$\leq 2 \times N_i + 1$	Hecht-Nielsen (1987)
$(N_i + N_O)/2$	Ripley (1993)
$2N_i/3$	Wang (1994)
$\sqrt{N_i \times N_O}$	Masters (1994)
$2N_i$	Kaastra and Boyd (1996), Kanellopoulas and Wilkinson (1997)

N_i number of input neurons, N_O number of output neurons

determine the optimal network architecture. According to Hornik et al. (1989), a network with one hidden layer can approximate any continuous function. Therefore, one hidden layer was utilized in this study. Establishing the number of neurons in the hidden layer is the most critical task in the ANN architecture (Sonmez et al. 2006; Sonmez and Gokceoglu 2008). Different equations have been proposed to determine the number of neurons in hidden layers by several researchers, as tabulated in Table 7. According to this table, for the problem at hand, the number of

this manner, 80 % of the data sets were assigned for training purposes while the further 20 % was used for testing of the network performance. In order to obtain superior performance of the ANN model, it is necessary to

neurons that might be used in the hidden layer varies between 2 and 9. In order to determine the optimum number of neurons in the hidden layer, using the trial-error method, several networks with one hidden layer were trained and tested as tabulated in Tables 8 and 9 for the prediction of UCS and E, respectively. As shown in these tables, each model was iterated five times. These tables show the results in terms of R^2 and RMSE for the training and testing data sets. According to the presented results, model number 3 with four hidden nodes (second iteration) and model number 2 with three hidden nodes (4th iteration) indicate higher prediction performances for UCS and E, respectively, compared to other models. Therefore, these models, i.e., models 2 and 3, were chosen as the best ANN models for prediction of UCS and E, respectively. It should be mentioned that model performance was evaluated based on both training and testing data sets. It is also worth mentioning that in construction of ANN models, the learning rate and momentum coefficient were set to 0.05 and 0.9, respectively.

Adaptive neuro-fuzzy inference system

The ANFIS was developed by Jang (1993). This system is capable of approximating any actual continuous function at any accuracy level (Jang et al. 1997). Therefore, a functional mapping can be modeled by ANFIS that approximates the prediction process of the internal system parameter. ANFIS is an artificial intelligence method that integrates the FIS concept into the ANN and has been extensively utilized in the field of geotechnical engineering (Grima et al. 2000; Gokceoglu et al. 2004; Iphar et al. 2008; Yilmaz and Yuksek 2009; Sezer et al. 2014). Mapping relations between the input and output parameters through hybrid learning for the determination of the membership function distribution can be simulated by ANFIS. A typical ANFIS network architecture with two input variables (x, y) and one output (f) is shown in Fig. 3. It is comprised of five layers in the inference system, and each layer includes several nodes, which are defined by the node function.

For previous layers, the output neuron is identified as the input signal in the present layer. After manipulation by the node function in the present layer, the output will serve as input signal for the next layer. To describe the procedure of ANFIS in brief, x and y as inputs and f as output are considered in the FIS models. Therefore, two fuzzy "if-then" rules can be constructed as follows (Takagi and Sugeno 1985):

If x is $A1$ and y is $B1$ then $f1 = p1x + q1y + r1$, (rule 1)

If x is $A2$ and y is $B2$ then $f2 = p2x + q2y + r2$, (rule 2)

where A_1, A_2, B_1 and B_2 are the membership functions for inputs x and y; p_1, q_1, r_1, p_2, q_2 and r_2 are the parameters of

Table 8 Performances of trained ANN models in predicting UCS

Model no.	Nodes in hidden layers	Network result																		
		Iteration 1				Iteration 2				Iteration 3				Iteration 4				Iteration 5			
		Train		Test		Train		Test		Train		Test		Train		Test		Train		Test	
		R^2	RMSE	R^2	RMSE	R^2	RMSE	R^2	RMSE	R^2	RMSE	R^2	RMSE	R^2	RMSE	R^2	RMSE	R^2	RMSE	R^2	RMSE
1	2	0.863	16.166	0.885	15.424	0.841	16.765	0.901	15.724	0.803	18.236	0.865	15.964	0.793	19.576	0.794	20.409	0.808	16.043	0.895	15.094
2	3	0.889	15.654	0.804	16.444	0.896	15.137	0.871	16.129	0.832	16.897	0.784	17.834	0.767	18.166	0.815	15.960	0.761	18.520	0.805	15.004
3	4	0.877	16.210	0.849	14.780	0.912	13.544	0.906	12.573	0.819	16.190	0.855	16.003	0.822	16.810	0.865	16.450	0.890	14.555	0.806	15.874
4	5	0.781	21.120	0.846	15.780	0.753	19.006	0.675	21.423	0.901	14.110	0.866	15.422	0.818	17.226	0.909	14.104	0.733	20.092	0.811	16.984
5	6	0.839	15.876	0.715	19.494	0.888	16.166	0.885	15.984	0.814	16.777	0.829	15.654	0.907	15.096	0.844	16.220	0.855	16.446	0.811	17.464
6	7	0.848	16.781	0.801	17.410	0.788	19.186	0.831	15.889	0.718	16.166	0.810	15.736	0.887	15.225	0.868	15.477	0.849	16.106	0.672	20.558
7	8	0.902	14.641	0.877	15.894	0.713	19.109	0.635	21.702	0.895	15.144	0.830	15.886	0.680	21.776	0.895	14.980	0.880	15.463	0.882	15.453
8	9	0.899	15.136	0.869	15.701	0.844	16.635	0.867	15.551	0.892	15.344	0.860	15.789	0.742	20.966	0.765	21.664	0.760	19.747	0.688	21.455

Table 9 Performances of trained ANN models in predicting E

Model no.	Nodes in hidden layers	Network result																			
		Iteration 1				Iteration 2				Iteration 3				Iteration 4				Iteration 5			
		Train		Test		Train		Test		Train		Test		Train		Test		Train		Test	
		R^2	RMSE	R^2	RMSE	R^2	RMSE	R^2	RMSE	R^2	RMSE	R^2	RMSE	R^2	RMSE	R^2	RMSE	R^2	RMSE	R^2	RMSE
1	2	0.898	13.566	0.920	9.897	0.875	15.105	0.903	11.167	0.843	16.431	0.908	11.384	0.809	17.618	0.810	16.368	0.824	14.439	0.913	10.585
2	3	0.925	10.104	0.836	14.816	0.920	9.638	0.915	9.532	0.874	15.224	0.823	15.068	0.927	8.712	0.918	9.187	0.896	13.668	0.899	12.504
3	4	0.912	10.605	0.883	13.317	0.923	9.203	0.909	11.328	0.860	14.587	0.898	14.419	0.838	15.129	0.882	14.805	0.815	15.108	0.822	14.287
4	5	0.812	15.029	0.880	14.218	0.783	16.124	0.709	19.302	0.916	12.713	0.909	10.895	0.834	15.503	0.917	12.694	0.748	17.083	0.827	15.286
5	6	0.873	14.304	0.744	17.564	0.924	10.166	0.910	10.402	0.855	15.116	0.870	14.104	0.925	8.886	0.861	14.598	0.872	14.801	0.827	15.718
6	7	0.882	15.120	0.833	15.686	0.820	15.287	0.873	14.316	0.754	14.566	0.851	14.178	0.905	10.703	0.885	13.929	0.866	14.495	0.685	18.502
7	8	0.912	11.192	0.914	11.320	0.742	17.217	0.667	19.554	0.911	13.645	0.872	14.313	0.694	18.598	0.913	13.482	0.901	13.917	0.900	13.908
8	9	0.915	9.638	0.904	11.147	0.878	14.988	0.910	11.011	0.871	13.825	0.903	11.226	0.757	17.869	0.780	19.498	0.775	17.772	0.702	19.310

the output function. In the following, the five-layer ANFIS including two fuzzy rules, x and y (inputs), and one output (f) is presented (Jang 1993; Jang et al. 1997):

Layer 1 All nodes i in this layer are adaptive nodes:

$$O_{1,i} = \mu A_i(x), \tag{9}$$

$$O_{1,i} = \mu B_i(y), \tag{10}$$

for $i = 1, 2$ where x and y are considered as input neurons, and A and B are the linguistic labels. Also, $\mu A_i(x)$ and $\mu B_i(y)$ are the membership functions.

Layer 2 The nodes are labeled Π and identified by a circle. The output neuron is created by all the incoming signals:

$$O_{2,i} = \omega_i = \mu A_i(x)\,\mu B_i(y) \text{ with } i = 1, 2. \tag{11}$$

The output neuron ω_i presents the firing strength of a rule.

Layer 3 Every node in this layer is a fixed node to be marked by a circle and labeled as N. The output is computed by the ratio of the ith rule's firing strength over the sum of all rules' firing strength:

$$O_{3,i} = \varpi_i = \omega_i/(\omega_1 + \omega_2) \text{ with } i = 1, 2. \tag{12}$$

Layer 4 In this layer, every node is an adaptive node with the node function as follows:

$$O_{4,i} = \varpi_i f_i = \varpi_i(p_i x + q_i y + r_i), \tag{13}$$

where parameters p_i, q_i and r_i are named the consequent parameters. A normalized firing strength is named ϖ_i.

Layer 5 In this layer (final step), the output amount is created by the sum of all incoming signals:

$$O_{5,i} = \sum_i \varpi_i f_i = \sum_i \varpi_i f_i / \sum_i \varpi_i; i = 1, 2. \tag{14}$$

BP gradient descent is the basic learning rule of the ANFIS, which computes error signals recursively from the output layer backward to the input nodes. Based on the architecture in Fig. 3b, the output (f) can be stated as a linear combination of the consequent parameters. To learn the fuzzy model employing differentiable functions, the ANFIS utilizes a hybrid-learning rule as it is easy to use. The classical BP technique is used by the ANFIS to learn the parameters of membership functions. Also, the conventional least-squares predictor is applied by the ANFIS to learn the parameter of the first-order polynomial of the Takagi-Sugeno-Kang fuzzy model (Jang et al. 1997).

In the procedure of the ANFIS, there are two different passes of hybrid learning (forward and backward). In the forward pass, functional signals go forward until the fourth layer, and the consequent parameters are investigated by the least-squares estimate. Similar to the ANN procedure, the system errors are propagated back and the premise parameters are updated using the gradient descent in the backward pass. The final output can be defined as follows:

Fig. 3 **a** First order Sugeno fuzzy reasoning; **b** equivalent ANFIS architecture (following Jang et al. 1997)
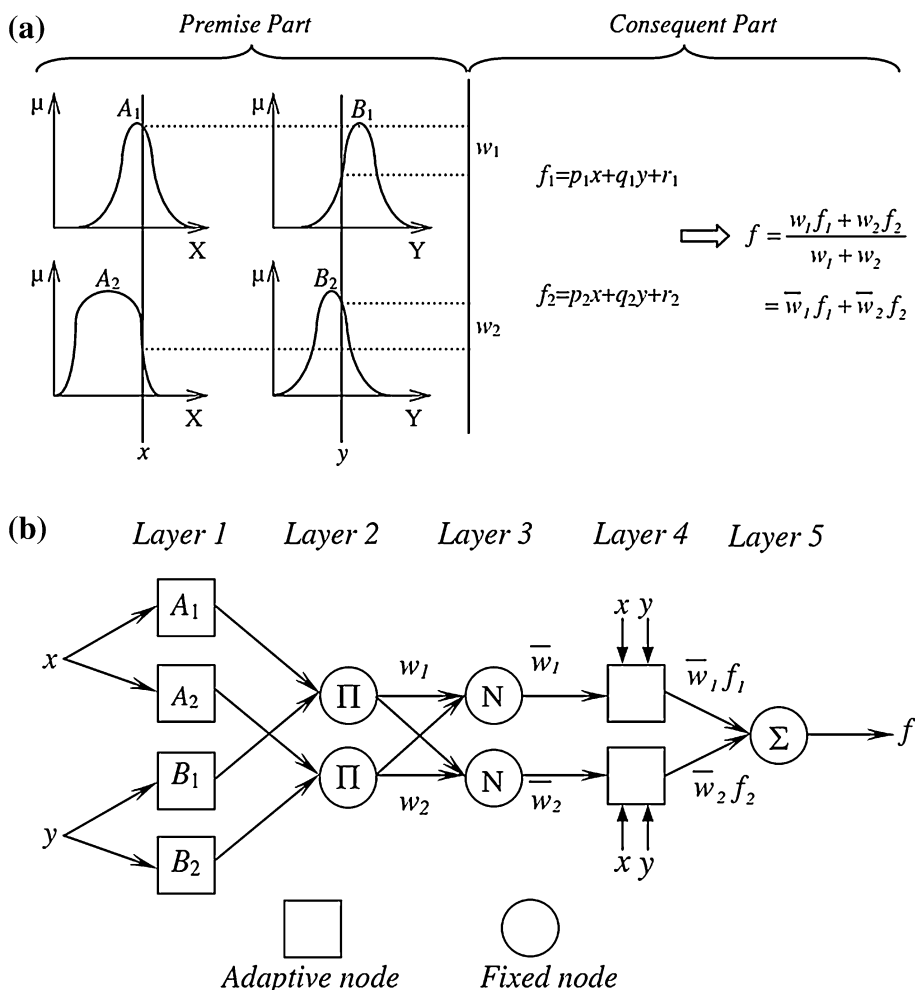
$$f = \frac{\omega_1}{\omega_1 + \omega_2}f_1 + \frac{\omega_1}{\omega_1 + \omega_2}f_2$$
$$= \varpi_1(p_1x + q_1y + r_1) + \varpi_2(p_2x + q_2y + r_2)$$
$$= (\varpi_1x)p_1 + (\varpi_1y)q_1 + (\varpi_1)r_1 + (\varpi_2x)p_2 + (\varpi_2y)q_2$$
$$+ (\varpi_2)r_2, \tag{15}$$

in which p_1, q_1, r_1, p_2, q_2 and r_2 are consequent parameters. The advantage of using the ANFIS model is that the consequent parameters and optimal premise parameters can be efficiently obtained in the learning process.

In this study, a hybrid intelligent system (ANFIS) for predicting UCS and E of granite was also applied. Similar to the ANN analyses part, all data sets were distributed randomly to training (80 %) and testing (20 %) data sets. In fact the idea behind using the testing data set is to verify the generalization capability of the proposed neural network model. The use of the random sampling procedure has been reported in several studies (Alvarez and Babuska 1999; Singh et al. 2001; Rabbani et al. 2012; Tonnizam Mohamad et al. 2014). In order to determine the number of fuzzy rules, using a trial-error method, many models of the

fuzzy rule combinations (e.g., 2 and 3) were employed for the UCS and E data sets separately. Eventually, it was found that input parameters with three fuzzy rules outperform the other ANFIS models for both UCS and E prediction. For the ANFIS modeling part, to select the optimum number of fuzzy rules, a parametric study was conducted. It was found that a number of 81 fuzzy rules ($3 \times 3 \times 3 \times 3$) shows the best performance in predicting UCS and E. However, Table 10 shows parameter types and their values used in the ANFIS model. In the next step of the modeling, ANFIS models were constructed to predict UCS and E. Prediction performance of these two outputs are presented in Table 11. As shown in these tables, each model was repeated five times using different training and testing data sets. Based on the tabulated results in this table, considering the results of both the training and testing data sets, model number 3 for UCS prediction and model number 4 for E prediction indicate higher prediction performances among all five models. Therefore, model number 3 and model number 4 were selected for prediction of UCS and E respectively. In this study, all ANFIS models

were trained by utilizing 100 epochs. The assigned membership functions with categories of low, medium and high for the best models of UCS and E are shown in Figs. 4, 5, 6 and 7. It is worth mentioning that these membership functions were assigned after the ANFIS training stage. Moreover, a linear type of membership function was used for the output (UCS and E). In order to estimate the membership functions parameters, a hybrid optimization method was utilized. It should be noted that all ANN and

Table 10 Different parameters used in ANFIS model

ANFIS parameter	Value
Input membership function	Gaussianmf
Output membership function	Linear
Number of nodes	193
Number of linear parameters	405
Number of nonlinear parameters	24
Total number of parameters	429
Number of training data pairs	36
Number of testing data pairs	9
Number of fuzzy rules	81

ANFIS models used to predict UCS and E were trained with the help of MATLAB version 7.14.0.739. Additionally, SPSS 18.0 was utilized for RMSE and statistical calculations.

Results and discussion

In this study an attempt has been made to show the capability of the MRA, ANN and ANFIS models to predict the UCS and E of granite. The models of ANFIS, ANN and MRA, for the prediction of UCS and E, were constructed using four inputs (ρ_{dry}, V_p, Qtz and Plg) and two outputs. The graph of predicted UCS and E using the MRA technique against the measured UCS and E for all 45 samples is displayed in Fig. 8. As indicated in this figure, the relatively low R^2 values, equal to 0.545 and 0.667, reveal the low reliability of the MRA technique for prediction of UCS and E ,respectively. Figures 9 and 10 show the predicted UCS and E by employing an ANN model plotted against the measured UCS and E values for the training and testing data sets, respectively. The R^2 values of 0.912 and 0.906 for the training and testing of UCS prediction and also

Table 11 Performances of the five ANFIS models in predicting UCS and E

| ANFIS model	UCS				E			
	Train		Test		Train		Test	
	R^2	RMSE	R^2	RMSE	R^2	RMSE	R^2	RMSE
1	0.965	7.881	0.983	6.560	0.977	3.919	0.973	4.873
2	0.979	7.021	0.972	6.932	0.969	4.091	0.961	4.322
3	0.985	6.373	0.994	5.590	0.988	3.552	0.971	4.677
4	0.981	6.702	0.994	5.772	0.987	3.350	0.995	4.053
5	0.954	7.844	0.968	6.981	0.972	4.230	0.978	4.619

Fig. 4 Assigned membership functions for the ρ_{dry} input parameter
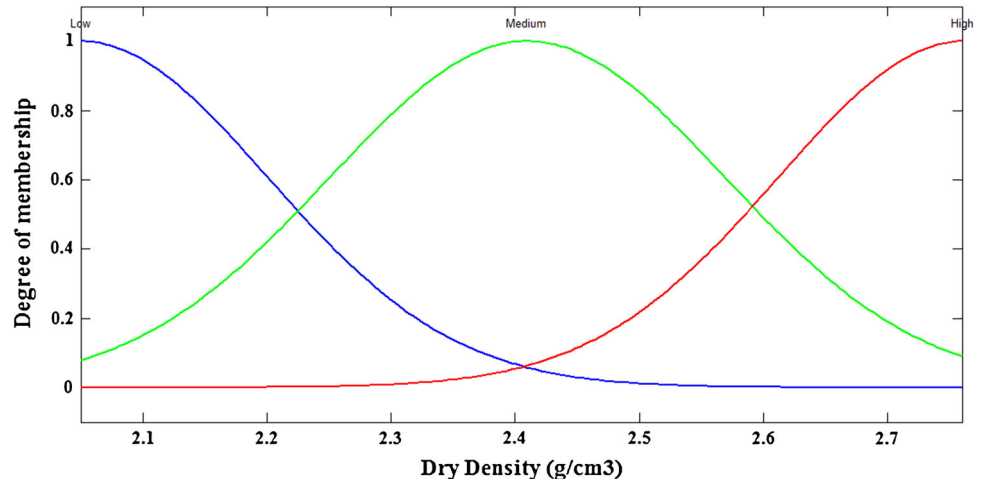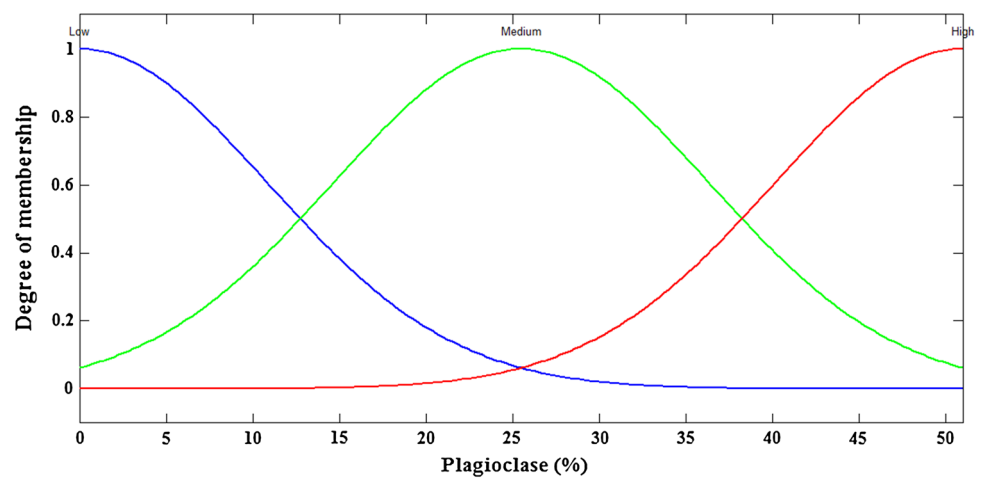
Fig. 5 Assigned membership functions for the V_p input parameter
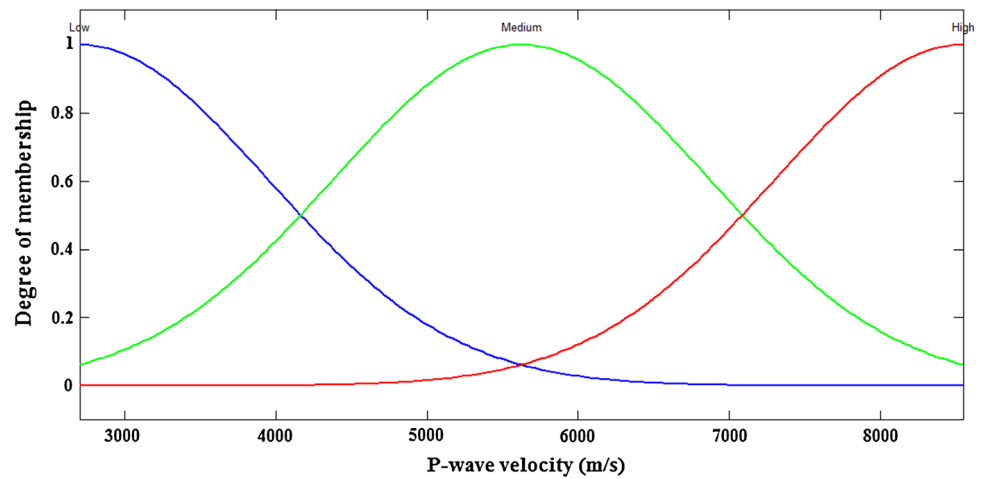
Fig. 6 Assigned membership functions for the Qtz input parameter
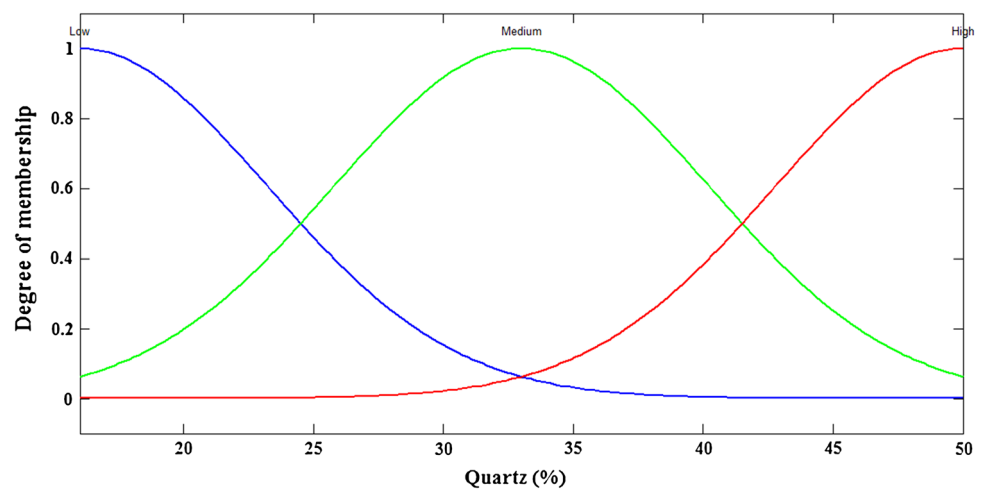
Fig. 7 Assigned membership functions for the Plg input parameter

0.927 and 0.918 for training and testing of the E prediction show that the ANN approach is able to predict UCS and E with relatively suitable accuracy. Furthermore, in the prediction of UCS and E using the ANFIS model, R^2 values of 0.985 and 0.994 for the training and testing of UCS and 0.987 and 0.995 for the training and testing of E suggest the
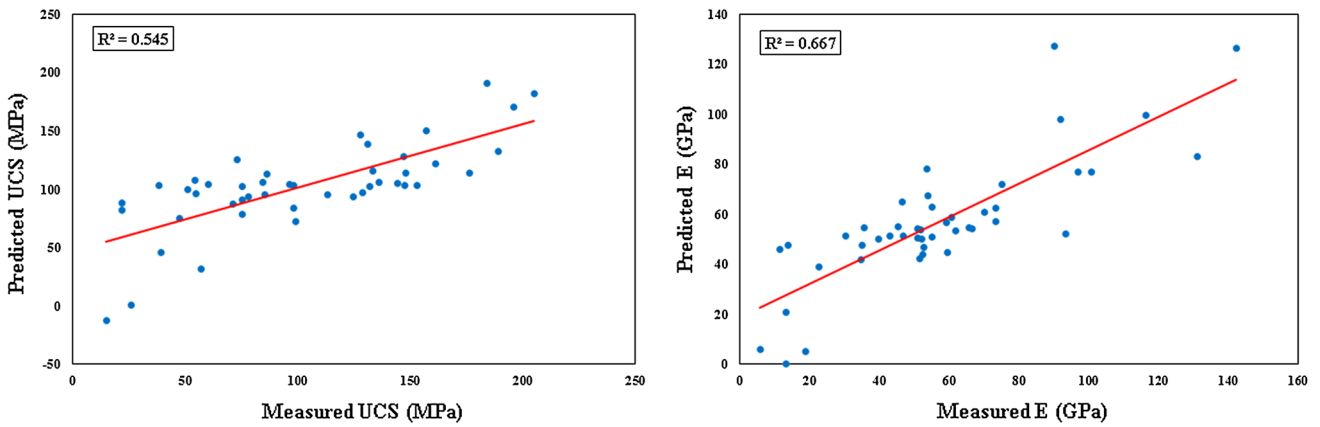
Fig. 8 R^2 of measured and predicted values of UCS and E using the MRA model
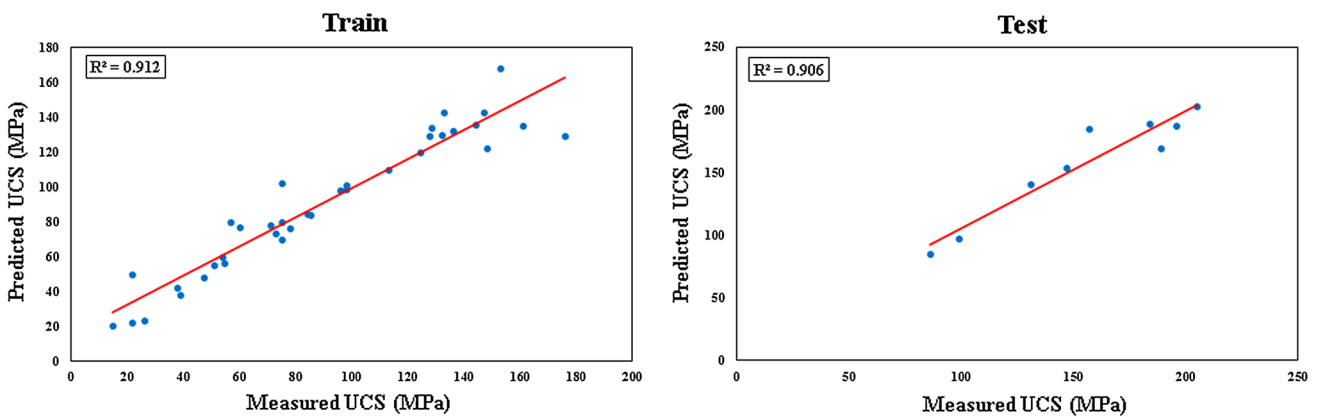
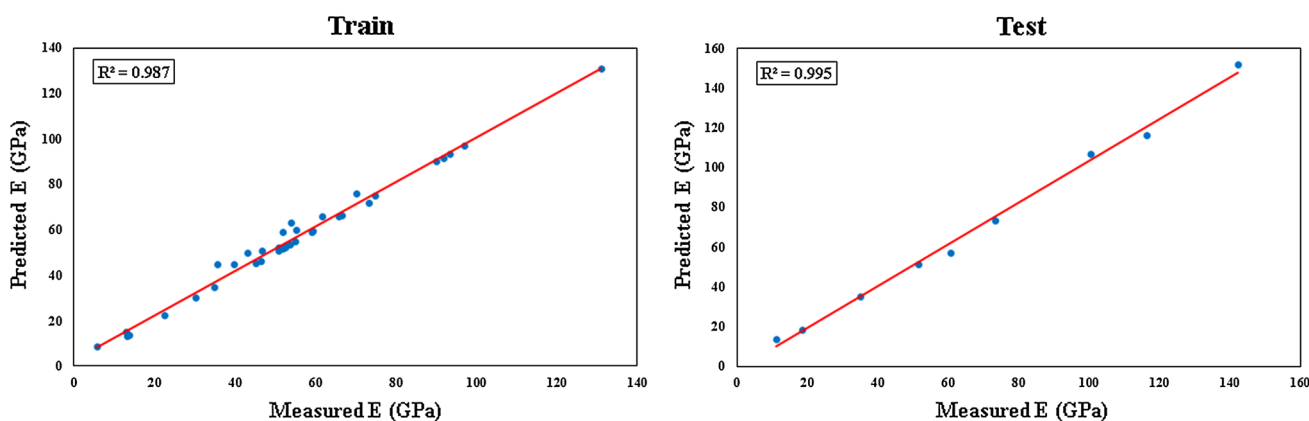**Fig. 9** R^2 values of the measured and predicted UCS for training and testing data sets using the ANN model
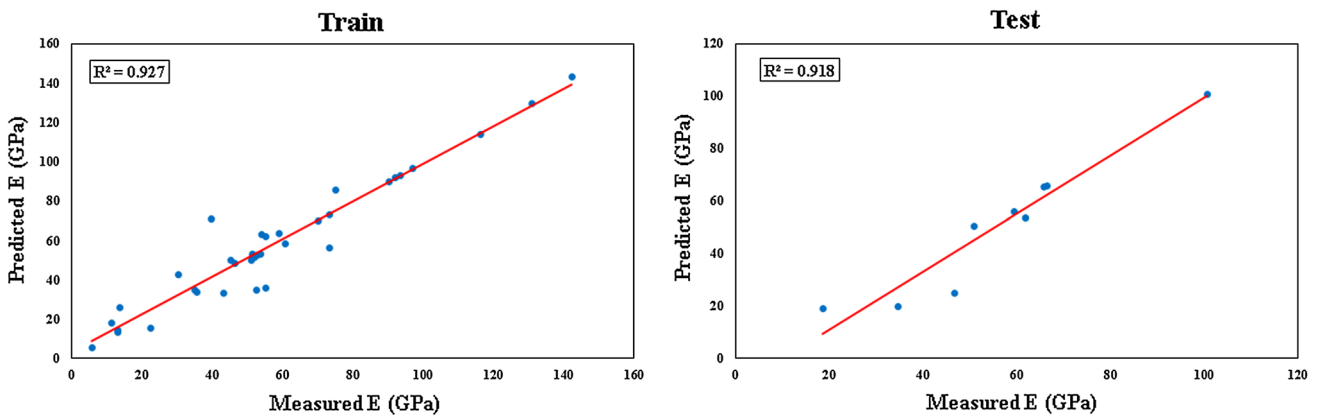
Fig. 10 R^2 values of the measured and predicted E for the training and testing data sets using the ANN model

superiority of this model in predicting the UCS and E of granite (see Figs. 11, 12).

In this study, the RMSE and amount of value account for (VAF) were computed to control the capacity performance of the predictive models developed, as applied by Alvarez and Babuska (1999) and Gokceoglu (2002):

$$\text{RMSE} = \sqrt{\frac{1}{N}\sum_{i=1}^{N}(y - y')^2}, \tag{16}$$

$$\text{VAF} = \left[1 - \frac{\text{var}(y - y')}{\text{var}(y)}\right] \times 100, \tag{17}$$
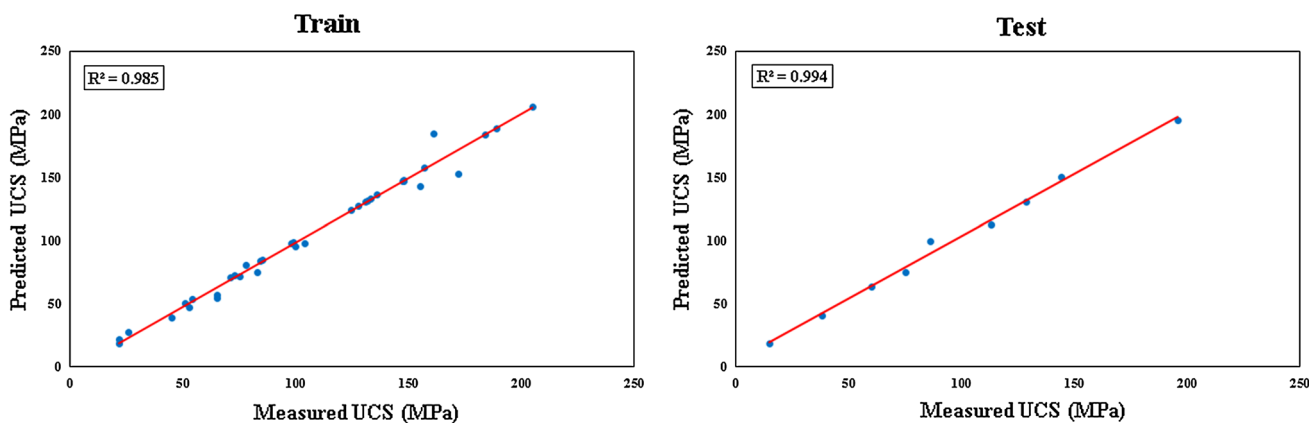
Fig. 11 R^2 values of the measured and predicted UCS for the training and testing data sets using the ANFIS model

Fig. 12 R^2 values of the measured and predicted E for the training and testing data sets using the ANFIS model

Table 12 Performance indices of the predictive models for all 45 data sets

Predictive model	UCS			E		
	R^2	RMSE	VAF (%)	R^2	RMSE	VAF (%)
MRA	0.545	34.197	54.505	0.667	17.418	66.682
ANN	0.911	13.355	91.098	0.919	8.809	91.496
ANFIS	0.985	6.224	98.455	0.990	3.503	98.968

where y and y' are the obtained and estimated values, respectively, and N is the total number of data. The model is excellent if the RMSE is zero and VAF is 100. Performance indices obtained by predictive models for all 45 data sets are shown in Table 12. As tabulated in this table, the ANFIS predictive model can provide higher performance in the prediction of UCS and E in comparison to other predictive models. In order to demonstrate a better comparison, the RMSE and VAF values for predictive models are displayed in Fig. 13. According to this figure, the

RMSE and VAF values reveal that the performance capacity of the ANFIS predictive model is higher than that of both the MRA and ANN predictive models.

The results demonstrate that all aforementioned models are applicable when predicting the UCS and E of granite. However, these approaches should be used according to the situation. The ANFIS predictive model may be used when a high degree of accuracy is required. Moreover, the MRA predictive model can be used in conditions where a simple estimation of UCS and E is desired.

Conclusion

A total of 45 granite rock samples were collected during site investigation of the Pahang-Selangor raw water transfer tunnel to predict their UCS and E values. Subsequently, MRA, ANN and ANFIS predictive models were applied to predict UCS and E using four inputs: ρ_{dry}, ultrasonic velocity, Qtz content and Plg. Prediction results showed that the ANFIS predictive model can predict UCS and
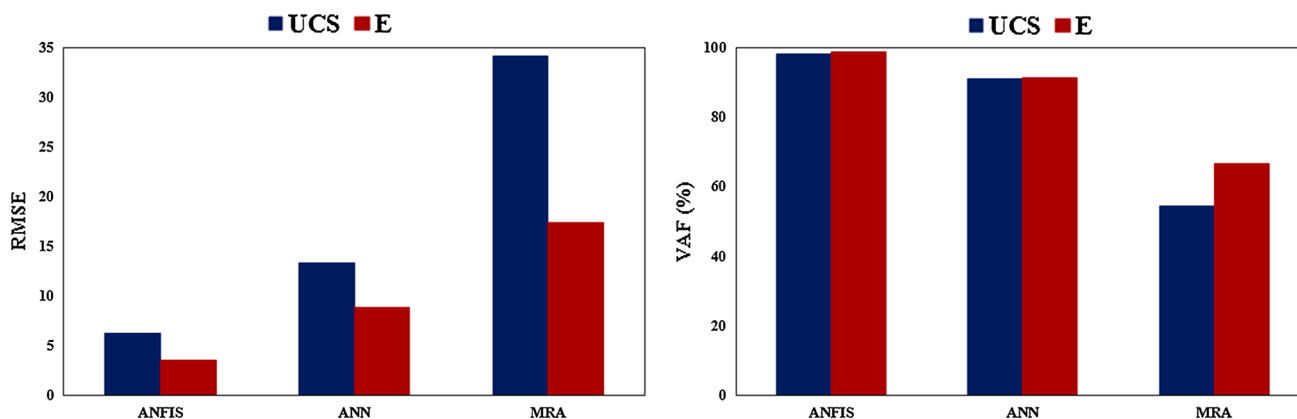
Fig. 13 Comparison of the RMSE and VAF values for MRA, ANN and ANFIS predictive models

E much better than the ANN and MRA predictive models. The R^2 values (for all data sets) equal to 0.985 and 0.990 for UCS and E, respectively, express the high reliability of the ANFIS predictive model, while these values were 0.911 and 0.919 for the ANN model and 0.545 and 0.667 for the MRA model. Nevertheless, these predictive models can be applied to predict UCS and E depending on the situation. In terms of performance, it was also shown that using ANFIS constitutes a feasible approach to minimizing uncertainties when designing rock engineering projects. The ANFIS displays several benefits as it combines the advantages of ANN and FIS techniques to demonstrate a high prediction capacity in complex, nonlinear and multivariable engineering problems.

References

Alvarez GM, Babuska R (1999) Fuzzy model for the prediction of unconfined compressive strength of rock samples. Int J Rock Mech Min Sci 36:339–349

Asadi M, Hossein Bagheripour M, Eftekhari M (2013) Development of optimal fuzzy models for predicting the strength of intact rocks. Comput Geosci 54:107–112

Atici U (2011) Prediction of the strength of mineral admixture concrete using multivariable regression analysis and an artificial neural network. Expert Syst Appl 38:9609–9618

Basu A, Aydin A (2006) Predicting uniaxial compressive strength by point load test: significance of cone penetration. Rock Mech Rock Eng 39:483–490

Beiki M, Majdi A, Givshad AD (2013) Application of genetic programming to predict the uniaxial compressive strength and elastic modulus of carbonate rocks. Int J Rock Mech Min Sci 63:159–169

Ceryan N, Okkan U, Kesimal A (2012) Prediction of unconfined compressive strength of carbonate rocks using artificial neural networks. Environ Earth Sci 68(3):807–819

Cevik A, Sezer EA, Cabalar AF, Gokceoglu C (2011) Modeling of the uniaxial compressive strength of some clay-bearing rocks using neural network. Appl Soft Comput 11(2):2587–2594

Cobanglu I, Celik S (2008) Estimation of uniaxial compressive strength from point load strength, Schmidt hardness and P-wave velocity. Bull Eng Geol Environ 67:491–498

Dehghan S, Sattari GH, Chehreh CS, Aliabadi MA (2010) Prediction of unconfined compressive strength and modulus of elasticity for Travertine samples using regression and artificial neural networks. Min Sci Technol 20:0041–0046

Dreyfus G (2005) Neural networks: methodology and application. Springer, Berlin

Garret JH (1994) Where and why artificial neural networks are applicable in civil engineering. J Comput Civil Eng 8:129–130

Gokceoglu C (2002) A fuzzy triangular chart to predict the uniaxial compressive strength of the Ankara agglomerates from their petrographic composition. Eng Geol 66(1):39–51

Gokceoglu C, Zorlu K (2004) A fuzzy model to predict the unconfined compressive strength and modulus of elasticity of a problematic rock. Eng Appl Artif Intell 17:61–72

Gokceoglu C, Yesilnacar E, Sonmez H, Kayabasi A (2004) A neurofuzzy model for modulus of deformation of jointed rock masses. Comput Geotech 31(5):375–383

Grima MA, Bruines PA, Verhoef PNW (2000) Modeling tunnel boring machine performance by neuro-fuzzy methods. Tunn Undergr Space Technol 15(3):260–269

Hajihassani M, Jahed Armaghani D, Sohaei H, Tonnizam Mohamad E, Marto A (2014) Prediction of airblast-overpressure induced by blasting using a hybrid artificial neural network and particle swarm optimization. Appl Acoust 80:57–67

Hecht-Nielsen R (1987) Kolmogorov's mapping neural network existence theorem. In: Proceedings of the first IEEE international conference on neural networks, San Diego CA, USA, pp 11–14

Hornik K, Stinchcombe M, White H (1989) Multilayer feedforward networks are universal approximators. Neural Netw 2:359–366

Iphar M, Yavuz M, Ak H (2008) Prediction of ground vibrations resulting from the blasting operations in an open-pit mine by adaptive neuro-fuzzy inference system. Environ Geol 56:97–107

ISRM (2007) The complete ISRM suggested methods for rock characterization, testing and monitoring: 1974–2006. In: Ulusay R, Hudson JA (eds) Suggested methods prepared by the commission on testing methods, International Society for Rock Mechanics

Jahed Armaghani D, Hajihassani M, Yazdani Bejarbaneh B, Marto A, Tonnizam Mohamad E (2014) Indirect measure of shale shear strength parameters by means of rock index tests through an optimized artificial neural network. Measurement 55:487–498

JahedArmaghani D, Hajihassani M, Mohamad ET, Marto A, Noorani SA (2013) Blasting-induced flyrock and ground vibration prediction through an expert artificial neural network based on particle swarm optimization. Arab J Geosci. doi:10.1007/s12517-013-1174-0

Jang RJS (1993) Anfis: adaptive-network-based fuzzy inference system. IEEE Trans Syst Man Cybern 23:665–685

Jang RJS, Sun CT, Mizutani E (1997) Neuro-fuzzy and soft computing. Prentice-Hall, Upper Saddle River, p 614

Kaastra I, Boyd M (1996) Designing a neural network for forecasting financial and economic time series. Neurocomputing 10:215–236

Kahraman S (2001) Evaluation of simple methods for assessing the uniaxial compressive strength of rock. Int J Rock Mech Min Sci 38:981–994

Kahraman S (2014) The determination of uniaxial compressive strength from point load strength for pyroclastic rocks. Eng Geol 170:33–42

Kahraman S, Fener M, Kozman E (2012) Predicting the compressive and tensile strength of rocks from indentation hardness index. J S Afr Inst Min Metall 112(5):331–339

Kanellopoulas I, Wilkinson GG (1997) Strategies and best practice for neural network image classification. Int J Remote Sens 18:711–725

Karaman K, Kesimal A (2014) A comparative study of Schmidt hammer test methods for estimating the uniaxial compressive strength of rocks. Bull Eng Geol Environ. doi:10.1007/s10064-014-0617-5

Kosko B (1994) Neural networks and fuzzy systems: a dynamical systems approach to machine intelligence. Prentice Hall, New Delhi

Majdi A, Beiki M (2010) Evolving neural network using a genetic algorithm for predicting the deformation modulus of rock masses. Int J Rock Mech Min Sci 47(2):246–253

Marto A, Hajihassani M, Jahed Armaghani D, Tonnizam Mohamad E, Makhtar AM (2014) A novel approach for blast-induced flyrock prediction based on imperialist competitive algorithm and artificial neural network. Sci World J. Article ID 643715

Masters T (1994) Practical neural network recipes in C++. Academic Press, Boston

Meulenkamp F, Grima MA (1999) Application of neural networks for the prediction of the unconfined compressive strength (UCS) from Equotip hardness. Int J Rock Mech Min Sci 36(1):29–39

Mishra DA, Basu A (2013) Estimation of uniaxial compressive strength of rock materials by index tests using regression analysis and fuzzy inference system. Eng Geol 160:54–68

Momeni E, Nazir R, JahedArmaghani D, Maizir H (2014a) Prediction of pile bearing capacity using a hybrid genetic algorithm-based ANN. Measurement 57:122–131

Momeni E, Jahed Armaghani D, Hajihassani M, Mohd Amin MF (2014b) Prediction of uniaxial compressive strength of rock samples using hybrid particle swarm optimization-based artificial neural networks. Measurement .doi:10.1016/j.measurement.2014.09.075

Monjezi M, Khoshalan HA, Razifard M (2012) A neuro-genetic network for predicting uniaxial compressive strength of rocks. Geotech Geol Eng 30(4):1053–1062

Moradian ZA, Ghazvinian AH, Ahmadi M, Behnia M (2010) Predicting slake durability index of soft sandstone using indirect tests. Int J Rock Mech Min Sci 47(4):666–671

Nazir R, Momeni E, Jahed Armaghani D, Mohd Amin MF (2013a) Correlation between unconfined compressive strength and indirect tensile strength of limestone rock samples. Electr J Geotech Eng 18:1737–1746

Nazir R, Momeni E, JahedArmaghani D, Mohd Amin MF (2013b) Prediction of unconfined compressive strength of limestone rock samples using L-type Schmidt hammer. Electr J Geotech Eng 18:1767–1775

O'Rourke JE (1989) Rock index properties for geoengineering in underground development. Miner Eng 106–110

Rabbani E, Sharif F, KoolivandSalooki M, Moradzadeh A (2012) Application of neural network technique for prediction of uniaxial compressive strength using reservoir formation properties. Int J Rock Mech Min Sci 56:100–111

Rezaei M, Majdi A, Monjezi M (2012) An intelligent approach to predict unconfined compressive strength of rock surrounding access tunnels in longwall coal mining. Neural Comput Appl 24(1):233–241

Ripley BD (1993) Statistical aspects of neural networks. In: Barndoff-Neilsen OE, Jensen JL, Kendall WS (eds) Networks and chaos-statistical and probabilistic aspects. Chapman & Hall, London, pp 40–123

Sezer EA, Nefeslioglu HA, Gokceoglu C (2014) An assessment on producing synthetic samples by fuzzy C-means for limited number of data in prediction models. Appl Soft Comput 24:126–134

Simpson PK (1990) Artificial neural system: foundation, paradigms, applications and implementations. Pergamon, New York

Singh RN, Hassani FP, Elkington PAS (1983) The application of strength and deformation index testing to the stability assessment of coal measures excavations. In: Proceeding of 24th US symposium on rock mechanism, Texas A and M Univ. AEG, Balkema, Rotterdam, pp 599–609

Singh VK, Singh D, Singh TN (2001) Prediction of strength properties of some schistose rocks from petrographic properties using artificial neural networks. Int J Rock Mech Min Sci 38(2):269–284

Singh R, Kainthola A, Singh TN (2012) Estimation of elastic constant of rocks using an ANFIS approach. Appl Soft Comput 12(1):40–45

Sonmez H, Gokceoglu C (2008) Discussion on the paper by H. Gullu and E. Ercelebi, "A neural network approach for attenuation relationships: an application using strong ground motion data from Turkey. Eng Geol 97:91–93

Sonmez H, Tuncay E, Gokceoglu C (2004) Models to predict the uniaxial compressive strength and the modulus of elasticity for Ankara Agglomerate. Int J Rock Mech Min Sci 41(5):717–729

Sonmez H, Gokceoglu C, Nefeslioglu HA, Kayabasi A (2006) Estimation of rock modulus: for intact rocks with an artificial neural network and for rock masses with a new empirical equation. Int J Rock Mech Min Sci 43:224–235

Sulukcu S, Ulusay R (2001) Evaluation of the block punch index test with particular reference to the size effect, failure mechanism and its effectiveness in predicting rock strength. Int J Rock Mech Min Sci 38:1091–1111

Takagi T, Sugeno M (1985) Fuzzy identification of systems and its applications to modeling and control. IEEE Trans Syst Man Cybern 15:116–132

Tandon RS, Gupta V (2014) Estimation of strength characteristics of different Himalayan rocks from Schmidt hammer rebound, point load index, and compressional wave velocity. Bull Eng Geol Environ. doi:10.1007/s10064-014-0629-1

Tawadrous AS, Katsabanis PD (2007) Prediction of surface crown pillar stability using artificial neural networks. Int J Numer Anal Method 31(7):917–931

Tonnizam Mohamad E, Jahed Armaghani D, Momeni E, Alavi Nezhad Khalil Abad SV (2014) Prediction of the unconfined compressive strength of soft rocks: a PSO-based ANN approach. Bull Eng Geol Environ. doi:10.1007/s10064-014-0638-0

Wang C (1994) A theory of generalization in learning machines with neural application. PhD thesis, The University of Pennsylvania, USA

Yagiz S (2011) Correlation between slake durability and rock properties for some carbonate rocks. Bull Eng Geol Environ 70(3):377–383

Yagiz S, Sezer EA, Gokceoglu C (2012) Artificial neural networks and nonlinear regression techniques to assess the influence of slake durability cycles on the prediction of uniaxial compressive strength and modulus of elasticity for carbonate rocks. Int J Numer Anal Method 36(14):1636–1650

Yasar E, Erdogan Y (2004) Estimation of rock physiomechanical properties using hardness methods. Eng Geol 71:281–288

Yesiloglu-Gultekin N, Gokceoglu C, Sezer EA (2013) Prediction of uniaxial compressive strength of granitic rocks by various nonlinear tools and comparison of their performances. Int J Rock Mech Min Sci 62:113–122

Yilmaz I, Sendir H (2002) Correlation of Schmidt hardness with unconfined compressive strength and Young's modulus in gypsum from Sivas (Turkey). Eng Geol 66(3):211–219

Yilmaz I, Yuksek G (2009) Prediction of the strength and elasticity modulus of gypsum using multiple regression, ANN, and ANFIS models. Int J Rock Mech Min Sci 46(4):803–810

Zorlu K, Gokceoglu C, Ocakoglu F, Nefeslioglu HA, Acikalin S (2008) Prediction of uniaxial compressive strength of sandstones using petrography-based models. Eng Geol 96(3):141–158